Inorganica Chimica Acta 362 (2009) 1149–1157

Contents lists available at ScienceDirect

Inorganica Chimica Acta

journal homepage: www.elsevier.com/locate/ica

8-Quinolinolato complexes of ruthenium(II) and (III)

Chi-Fai Leung [a], Chun-Yuen Wong [a], Chi-Chiu Ko [a], Man-Chong Yuen [a], Wing-Tak Wong [b], Wai-Yeung Wong [c], Tai-Chu Lau [a,*]

[a] Department of Biology and Chemistry, City University of Hong Kong, Tat Chee Avenue, Kowloon Tong, Hong Kong, China
[b] Department of Chemistry, The University of Hong Kong, Pokfulam Road, Hong Kong, China
[c] Department of Chemistry, Hong Kong Baptist University, Waterloo Road, Kowloon Tong, Hong Kong, China

ARTICLE INFO

Article history:
Received 27 February 2008
Received in revised form 19 May 2008
Accepted 28 May 2008
Available online 4 June 2008

Keywords:
Ruthenium
8-Quinolinolate
Alkene
Nitrogen ligands

ABSTRACT

Reduction of RuQ_3 (**1a**, Q = 8-quinolinolato) with Zn/Hg in the presence of various π-acceptor ligands in ethanol affords RuQ_2L_2 (L_2 = (dimethylsulfoxide)$_2$ (**2**); (4-picoline)$_2$ (**3**); *N*,*N*′-dimethyl-1,4-diazabuta-1,3-diene, dab (**4**); cyclooctadiene, COD (**5**); norborna-2,5-diene, nbd (**6**)). Compound **6** is isolated as an equimolar mixture of *cis*,*trans* (**6a**) and *trans*,*cis* (**6b**) isomers, which can be separated by column chromatography. DFT calculations have been performed on **6a** and **6b**. Oxidation of **3** and **6b** affords the corresponding ruthenium(III) species **7** and **8**, respectively. The structures of **2**, **3**, **4** and **6** have been determined by X-ray crystallography.

1. Introduction

8-Hydroxyquinoline (HQ) and its derivatives are among the most versatile and useful ligands with a variety of applications [1]. They form stable complexes with most metals, and they have been used as complexing agents and organic precipitants for the separation of metal-ions from mixtures in analytical chemistry [2–4]. They are also used for the spectrophotometric analysis of metal ions. The luminescent properties of many complexes of 8-hydroxyquinoline have also made these ligands useful for the sensing of metal ions [5,6]. Electroluminescence from AlQ_3 and GaQ_3 has potential applications in organic light emitting devices (OLEDs) [7–15]. Rare-earth complexes such as ErQ_3, NdQ_3, YbQ_3 are also useful for infrared electroluminescence devices [16–19]. The luminescent properties of PtQ_2 and IrQ_2 make them useful photosensitizers in solar energy conversion and photocatalytic processes [20–22].

Although 8-quinolinolato complexes of many metals have been extensively studied, only a few complexes of ruthenium have been reported. These include RuQ_3 (HQ = 8-hydroxyquinone) [23], RuQ_2(COD) (COD = 1,5-cyclooctadiene) [24], $RuQ_2(PPh_3)_2$ [25], $[RuQ_2(PPh_3)_2]PF_6$ [25] and $[RuL_2(Q)]^+$ (L = 2,2′-bipyridine, 1,10-phenanthroline and its derivatives) [26], which were prepared by different methods.

We report herein a general, high-yield (>75%) synthetic method for a series of tris(8-quinolinolato)ruthenium(III) complexes, including RuQ_3 (**1a**), $Ru(Me\text{-}Q)_3$ (**1b**, Me-Q = 2-methyl-8-quinolinolato) and $Ru(Cl\text{-}Q)_3$ (**1c**, Cl-Q = 5-chloro-8-quinolinolato). These complexes are convenient starting materials for the preparation a variety of bis(8-quinolinolato)ruthenium(II) complexes containing π-acceptor ligands such as pyridine, alkene, dimethylsulfoxide and diazadiene. In the case of RuQ_2(nbd) (norbornadiene) both the *cis*,*trans* or *trans*,*cis* isomers have been isolated and structurally characterized. These two isomers have significantly different properties including redox potentials and energies of electronic transitions, and DFT calculations have been performed on these two complexes. Stable bis(8-quinolinolato)ruthenium(III) complexes containing 4-picoline or norbornadiene have also been isolated.

2. Experimental

2.1. Materials and physical measurements

$Ru(acac)_3$ [27] and bis(1,3-dimethylimidazolidin-2-ylidene) [28] were prepared according to literature methods. The 8-hydroxyquinoline ligands were purchased from Aldrich. Other chemicals were of reagent grade and used without further purification. IR spectra were obtained from KBr discs by using a Bomen MB-120 FTIR spectrophotometer. UV–Vis spectra were recorded on either a Perkin–Elmer Lamda 19 or a Shimadzu UV3100 spectrophotometer. ^1H NMR spectra were recorded on a Varian (300 MHz) FT-NMR spectrometer. The chemical shifts (δ ppm) were reported with reference to tetramethylsilane (TMS). Elemental analyses were done on an Elementar Vario EL Analyzer. Electrospray ionization mass spectra (ESI/MS) were obtained with a PE-SCIEX API 300

---

* Corresponding author. Tel.: +852 27887811; fax: +852 27887406.
E-mail address: bhtclau@cityu.edu.hk (T.-C. Lau).

0020-1693/$ - see front matter © 2008 Elsevier B.V. All rights reserved.
doi:10.1016/j.ica.2008.05.036

triple quadruple mass spectrometer. Cyclic voltammograms were recorded on a PAR model 273 potentiostat, using ferrocene (Fc) as internal reference. A glassy carbon disk working electrode and a $Ag/AgNO_3$ reference electrode were used. The supporting electrolyte was 0.1 M $[NBu^n_4]PF_6$ in CH_3CN. $[NBu^n_4]PF_6$ (Aldrich) was recrystallized three times from ethanol and dried *in vacuo* at 120 °C for 24 h before use. Acetonitrile was first refluxed over calcium hydride and then distilled under argon.

2.2. Synthesis of complexes

2.2.1. RuQ_3 (**1a**)

A solid mixture of $Ru(acac)_3$ (0.5 g, 1.26 mmol) and 8-hydroxyquinoline (HQ) (1 g, 6.89 mmol) was heated to a melt at 180 °C under argon for 1 d. After cooling to room temperature the green residue was washed with diethyl ether and the excess 8-hydroxyquinoline was recovered by sublimation. The residue was then dissolved in dichloromethane and purified by column chromatography (silica gel) with chloroform as the eluent. The green crystals of the compound were obtained by recrystallization from chloroform/*n*-hexane. Yield 0.52 g (78%). *Anal.* Calc. for $RuN_3O_3C_{27}H_{18}Cl$: C, 60.78; H, 3.40; N, 7.88. Found: C, 61.14; H, 3.24; N, 7.54%. UV–Vis ($CHCl_3$) λ_{max}, nm (ε, $M^{-1}\,cm^{-1}\,dm^{-3}$): 428 (14230), 341 (7490). IR (KBr, cm^{-1}): 1568, 1496, 1458, 1372, 1314, 1107.

2.2.2. $Ru(Me\text{-}Q)_3$ (**1b**)

Green needle-shaped crystals of the complex were obtained by a procedure similar to that for **1a** using 8-hydroxy-2-methylquinoline. Yield 0.53 g (73%). *Anal.* Calc. for $RuC_{30}H_{24}N_3O_3$: C, 62.60; H,4.20; N,7.30. Found: C, 63.01; H, 4.54; N, 7.56%. UV–Vis ($CHCl_3$) λ_{max}, nm (ε, $M^{-1}\,cm^{-1}\,dm^{-3}$) = 427 (9870), 352 (7240). IR (KBr, cm^{-1}): 1566, 1493, 1451, 1366, 1303, 1084.

2.2.3. $Ru(Cl\text{-}Q)_3$ (**1c**)

Green needle-shaped crystals of the complex were obtained by a procedure similar to that for **1a** using 5-chloro-8-hydroxyquinoline. Yield 0.61 g (76%). *Anal.* Calc. for $RuC_{27}H_{15}N_3O_3Cl_3$: C, 50.92; H,2.37; N,6.60. Found: C, 51.23; H, 2.60; N, 6.86%. UV–Vis ($CHCl_3$)λ_{max}, nm (ε, $M^{-1}\,cm^{-1}\,dm^{-3}$) = 443 (15200), 347 (8610). IR (KBr, cm^{-1}): 1563, 1492, 1452, 1362, 1303, 1084.

2.2.4. $RuQ_2(dmso)_2$ (**2**)

A mixture of **1a** (80 mg, 0.15 mmol), dimethylsulfoxide (1 ml) and a few pieces of zinc amalgam in ethanol (15 ml) was refluxed under argon for 18 h. The resulting yellow solution was filtered and diethyl ether (30 ml) was added to the filtrate. Yellow crystals were obtained on standing the solution at 0 °C for 12 h. Yield 46 mg (56%). *Anal.* Calc. for $RuC_{24}H_{24}O_4N_2S_2$: C, 48.42; H, 4.43; N, 5.14. Found: C, 48.56; H, 4.58; N, 5.06%. UV–Vis (CH_2Cl_2) λ_{max}, nm (ε, $M^{-1}\,cm^{-1}\,dm^{-3}$) = 347 (5470), 435 (4100). IR (KBr, cm^{-1}): 1078 (ν_{SO}), 2970 (ν_{CH}, dmso). ^1H NMR (300 MHz, $CDCl_3$): δ 2.66 (s, 6H, dmso), 2.97 (s, 6H, dmso), 6.87 (dd, $^3J_{HH}$ = 6.9 Hz, $^4J_{HH}$ = 0.9 Hz, 2H), 6.91(dd, $^3J_{HH}$ = 8.1 Hz, $^4J_{HH}$ = 1.2 Hz, 2H,), 7.30–7.36 (m, 4H), 8.10 (dd, $^3J_{HH}$ = 8.4 Hz, $^4J_{HH}$ = 1.2 Hz, 2H), 9.42 (dd, $^3J_{HH}$ = 4.8 Hz, $^4J_{HH}$ = 1.2 Hz, 2H).

2.2.5. $RuQ_2(pic)_2$ (**3**)

A mixture of **1a** (80 mg, 0.15 mmol), 4-picoline (1 ml) and a few pieces of zinc amalgam in ethanol (15 ml) was refluxed under argon for 18 h. The resulting green solid was filtered and washed with diethyl ether. Yield 66 mg (76%). Crystal suitable for X-ray crystallography were obtained by diffusion of *n*-hexane into a dichloromethane solution of the green solid at 4 °C. *Anal.* Calc. for $RuC_{30}H_{26}O_2N_4$: C, 62.59; H, 4.55; N, 9.74. Found: C, 62.85; H, 4.67; N, 9.90%. UV–Vis (CH_2Cl_2) λ_{max}, nm (ε, $M^{-1}\,cm^{-1}\,dm^{-3}$) = 300 (6790), 368 (6730), 410 (8020), 476 (17280). IR (KBr, cm^{-1}): 2960 (ν_{CH}, 4-picoline). ^1H NMR (300 MHz, $CDCl_3$): δ 2.19 (s, 6H, CH_3 of pic), 6.64 (d, $^3J_{HH}$ = 7.8 Hz, 2H, Q), 6.85 (d, $^3J_{HH}$ = 6.0 Hz, 4H, pic), 6.89 (d, $^3J_{HH}$ = 8.7 Hz, 2H, Q), 7.02 (d,$^3J_{HH}$ = 8.1 Hz, 2H, Q), 7.23 (d, $^3J_{HH}$ = 12.6, 2H, Q), 7.60 (d, $^3J_{HH}$ = 8.4 Hz, 2H, Q), 8.35 (d,$^3J_{HH}$ = 4.8 Hz, 2H, Q), 8.58 (d, $^3J_{HH}$ = 6.0 Hz, 4H, pic).

2.2.6. $RuQ_2(dab)$ (**4**)

A mixture of **1a** (80 mg, 0.15 mmol), bis(1,3-dimethylimidazolidin-2-ylidene) (30 mg, 0.15 mmol) and a few pieces of zinc amalgam in dichloromethane (15 ml) was refluxed under argon for 5 h. The resulting purple solution was stirred in air for 0.5 h to produce a red solution, which was then evaporated to dryness. The residue was dissolved in dichloromethane and loaded onto a silica gel column. Elution with acetone/dichloromethane (1:5) and slow evaporation of the resulting solution afforded red crystals suitable for X-ray crystallography. Yield 22 mg (32%). *Anal. Calc. for $RuC_{22}H_{20}N_4O_2$: C, 55.80; H, 4.26; N, 11.84. Found: C, 55.68; H, 4.55; N, 12.01%. UV–Vis (CH_2Cl_2)*λ_{max}, nm (ε, $M^{-1}\,cm^{-1}\,dm^{-3}$) = 529 (18400), 401 (13370). IR (KBr, cm^{-1}): 2953 and 2922 (ν_{CH}, dab). ^1H NMR (300 MHz, $CDCl_3$): δ 3.40 (s, 6H, CH_3 of dab), 6.85 (s, 2H, N=CH of dab), 6.96 (m, 2H, Q), 7.20 (m, 2H, Q), 7.30 (m, 2H, Q) 7.91 (m, 2H, Q), 8.46 (m, 4H, Q).

2.2.7. $Ru(Q)_2(COD)$ (**5**)

This was obtained by a procedure similar to that for **3** using 1,5-cyclooctadiene (1 ml). The yellow product was recrystallized from dichloromethane/diethyl ether. Yield 46 mg (61%). *Anal. Calc. for $RuC_{25}H_{20}O_2N_2$: C, 62.36; H, 4.16; N, 5.82. Found: C, 62.08; H, 4.10; N, 5.97%. UV–Vis (CH_2Cl_2)* λ_{max}, nm (ε, $M^{-1}\,cm^{-1}\,dm^{-3}$) = 351 (7300), 427 (9660). IR (KBr, cm^{-1}): 2960, 2915 (ν_{CH}, cod). ^1H NMR (300 MHz, $CDCl_3$): δ 2.31 (m, 4H, CH_2 of COD), 2.51 (m, 2H, CH_2 of COD), 2.75 (m, 2H, CH_2 of COD), 3.40 (m, 2H, =CH of COD), 4.45 (m, 2H, =CH of COD), 6.84 (m, 2H, Q), 7.14 (m, 2H, Q), 7.30 (m 2H, Q), 7.40 (m, 2H, Q), 7.85 (m, 2H, Q), 8.48 (m, 2H, Q).

2.2.8. *cis,trans*-$[Ru^{II}Q_2(nbd)]$ (**6a**) and *trans,cis*-$[Ru^{II}Q_2(nbd)]$ (**6b**)

A mixture containing **1a** (160 mg, 0.3 mmol), 2,5-norbornadiene (2 ml) and a few pieces of zinc amalgam in ethanol (15 ml) was refluxed under argon for 24 h. The resulting solution was filtered and slow evaporation of the filtrate afforded a mixture of red and yellow crystals. X-ray crystallography showed that the red crystals consist of an equimolar mixture of **6a** and **6b** co-crystallized together, whereas the yellow crystals consist of **6a** only. The red crystals were then dissolved in dichloromethane loaded onto a neutral alumina column. **6a** was obtained by elution with dichloromethane while **6b** was obtained by elution with dichloromethane/acetone (10:1).

The combined yield of the yellow compound **6a** is 61 mg (42%). *Anal. Calc. for $RuC_{26}H_{24}O_2N_2$: C, 62.36; H, 4.19; N, 5.82. Found: C, 62.64; H, 4.15, N, 5.91%. UV–Vis (CH_2Cl_2)* λ_{max}, nm (ε, $M^{-1}\,cm^{-1}\,dm^{-3}$) = 350 (1210), 427(1920). IR (KBr, cm^{-1}): 2950 (ν_{CH}, nbd). ^1H NMR (300 MHz, $CDCl_3$): δ 1.64 (s, 2H, CH_2 of nbd), 3.95 (m, 2H, =CH of nbd,), 4.14 (s, 2H, CH of nbd), 4.84 (m, 2H, =CH of nbd), 6.83 (dd, $^3J_{HH}$ = 7.8 Hz, $^4J_{HH}$ = 1.2 Hz, 2H, Q), 7.09 (m, 2H, Q), 7.30 (dd, $^3J_{HH}$ = 5.1 Hz, $^4J_{HH}$ = 1.2 Hz, 2H, Q), 7.39 (d, $^3J_{HH}$ = 7.8, 2H, Q^6), 7.80 (dd, $^3J_{HH}$ = 8.1Hz, $^4J_{HH}$ = 0.9Hz, 2H, Q), 8.45 (dd, $^3J_{HH}$ = 4.8 Hz, $^4J_{HH}$ = 1.5Hz, 2H, Q).

The yield of the red compound **6b** is 51 mg (35%). *Anal. Calc. for $RuC_{26}H_{24}O_2N_2$: C, 62.36; H, 4.19; N, 5.82. Found: C, 62.53; H, 4.01, N, 5.70%. UV–Vis (CH_2Cl_2),* λ_{max}, nm (ε, $M^{-1}\,cm^{-1}\,dm^{-3}$) = 357 (1030), 500 (1000). IR (KBr, cm^{-1}): 2950 (CH, nbd). ^1H NMR (300 MHz, $CDCl_3$): δ 1.64 (s, 2H, CH_2 of nbd), 3.85 (m, 2H, =CH of nbd), 3.95 (s, 2H, CH of nbd), 4.57 (m, 2H, =CH of nbd), 6.72 (d, $^3J_{HH}$ = 7.8 Hz, 2H, Q), 6.84 (d, $^3J_{HH}$ = 6.0 Hz, 2H, Q), 7.26 (d, $^3J_{HH}$ = 15.9 Hz, 2H, Q), 7.53 (m, 2H, Q), 8.21 (dd, $^3J_{HH}$ = 7.5 Hz, 2H, Q), 9.44 (dd, $^3J_{HH}$ = 5.7 Hz, 2H, Q^2). ESI-MS (CH_3OH) *m/z*: 481.5, $[M]^+$.

2.2.9. [$RuQ_2(pic)_2$]BPh_4 (**7**)

A solution of $FeCl_3 \cdot 6H_2O$ (68 mg, 0.25 mmol) in methanol (3 ml) was slowly added to a solution containing **3** (120 mg, 0.21 mmol) and $NaBPh_4$ (76 mg, 0.25 mmol) in methanol (10 ml). After stirring for 30 min the resulting dark green crystalline solid was filtered, washed with methanol and then with diethyl ether. Yield 133 mg (71%). *Anal. Calc. for* $RuBC_{49}H_{40}O_2N_2$*: C, 73.40; H, 4.99; N, 3.50. Found: C, 73.03; H, 4.96; N, 3.76. ESI/MS (*CH_3OH*) m/z*: 575.6, $[M]^+$.

2.2.10. [$Ru(Q)_2(nbd)$]BPh_4 (**8**)

This compound was prepared by the oxidation of **6a** (120 mg, 0.25 mmol) with $FeCl_3 \cdot 6H_2O$ (81 mg, 0.30 mmol) in the presence of $NaBPh_4$ (99 mg, 0.30 mmol), similar to that for **7**. Yield 150 mg (75%). *Anal. Calc. for* $RuBC_{49}H_{40}O_2N_2$*: C, 73.40; H, 5.04; N, 3.50. Found: C, 73.03; H, 4.96; N, 3.76%. ESI/MS (*CH_3OH*) m/z*: 481.5, $[M]^+$.

2.3. Crystal structure determination

Intensity data were collected at ambient temperature using a Bruker Smart 1000 CCD diffractometer with graphite-monochromated Mo Kα radiation ($\lambda = 0.71073$ Å) in the ω-scan mode. Details of the intensity data collection and crystal data are given in Table 1. Selected bond lengths and angles for **2**, **3**, **4** and **6** are given in Tables 2–5, respectively. The data were corrected for Lorentz and polarization effects. Absorption corrections by the ψ-scan method or an approximation by inter-image scaling were applied. The structures were resolved by Heavy-atom Patterson method [29] or direct methods (SIR92 [30] or SHELXS-86 [31]), and expanded using Fourier techniques (DIRDIF94 [32] or DIRDIF99 [33]). Hydrogen atoms are included but not refined. All calculations were performed using the Crystal Structure [34] or TEXSAN [35] crystallographic software package from Molecular Structure Corporation.

2.4. Computational methodology

Density functional theory (DFT) calculations were performed on the complexes **6a** and **6b**. Their electronic ground states were fully optimized from the X-ray determined geometries (without symmetry imposed) using Becke's three-parameter hybrid functional [36] with the Lee–Yang–Parr correlation functional [37] (B3LYP). Relativistic small effective core potential was employed for Ru atom [38] and its valence basis set was (8s, 7p, 6d)/[6s, 5p, 3d] with $Z = 16.0$. For H, C, N, and O atoms, the split valence with polarization basis sets 6-31G* were employed [39]. The DFT calculations were accomplished using the GAUSSIAN 03 program [40]. Tight SCF convergence (10^{-8} au) was used for all calculations. Charge Decomposition Analysis (CDA) [41] was performed to investigate

Table 2
Selected bond lengths (Å) and bond angles (°) of **2**

Bond	Bond length (Å)/bond angle (°)
Ru(1)–S(1)	2.224(5)
Ru(1)–S(2)	2.233(5)
Ru(1)–O(1)	2.077(12)
Ru(1)–O(2)	2.094(11)
Ru(1)–N(1)	2.07(1)
Ru(1)–N(2)	2.08(2)
S(1)–O(3)	1.481(12)
S(2)–O(4)	1.457(13)
O(1)–Ru(1)–N(1)	79.7(6)
O(2)–Ru(1)–N(2)	81.1(5)
S(1)–Ru(1)–S(2)	90.1(2)
N(1)–Ru(1)–N(2)	164.7(6)
O(1)–Ru(1)–O(2)	86.9(5)
Ru(1)–S(1)–O(3)	117.7(6)
Ru(1)–S(2)–O(4)	118.0(6)

Table 3
Selected bond lengths (Å) and angles (°) for **3**

Bond	Distance (Å)/angle (°)
Ru(1)–N(1)	2.024(5)
Ru(1)–N(2)	2.040(5)
Ru(1)–N(3)	2.079(5)
Ru(1)–N(4)	2.059(5)
Ru(1)–O(1)	2.080(4)
Ru(1)–O(2)	2.095(4)
O(1)–Ru(1)–N(1)	81.32(19)
O(2)–Ru(1)–N(2)	80.9(2)
N(3)–Ru(1)–N(4)	87.17(19)
N(1)–Ru(1)–N(2)	91.93(18)
N(2)–Ru(1)–N(3)	174.2(2)
N(1)–Ru(1)–N(4)	172.95(19)
O(1)–Ru(1)–O(2)	174.38(16)

Table 1
Crystallographic data for compound **2**, **3**, **4** and **6**

Compound	**2**	**3**	**4**	**6a + 6b**
Empirical formula	$C_{22}H_{24}N_2O_4RuS_2$	$C_{30}H_{26}N_4O_2Ru$	$C_{22}H_{20}N_4O_2Ru$	$C_{50}H_{42}N_4O_5Ru_2$
Formula weight	545.63	575.62	473.50	981.05
λ (Å)	0.7107	0.71073	0.71069	0.71073
T (°C)	25	25	25	28
Space group	*Pbca* (#61)	$P2_1/c$	$P\bar{1}$(#2)	$P\bar{1}$(#2)
a (Å)	19.554(3)	12.683(3)	8.156(1)	11.804(2)
b (Å)	10.648(2)	13.410(3)	10.962(2)	12.730(0)
c (Å)	26.059(4)	15.195(4)	11.859(2)	15.123(2)
α (°)		90	97.87(1)	106.12(1)
β (°)		100.869(4)	98.37(1)	111.81(1)
γ (°)		90	102.22(1)	92.82(1)
V (Å^3)	5425.8(16)	2538.1(11)	1009.7(3)	1992.8(5)
Z value	8	4	2	2
D_{calc} (g cm^{-1})	1.336	1.506	1.557	1.635
F_{000}	2224	1176	480	996
μ(Mo Kα) (cm^{-1})	7.58	6.53	8.02	8.154
R^a	0.048	0.054	0.036	0.0259
Rw^b	0.087	0.129	0.048	0.0301
Goodness of fit	1.00	0.839	1.39	1.003

[a] $R = \sum||F_o| - |F_c||/\sum|F_o|$.
[b] $R_\omega = [\sum\omega(|F_o| - |F_c)^2/\sum\omega(F_o)]^{1/2}$.

Table 4
Selected bond lengths (Å) and bond angles (°) of **4**

Bond	Bond length (Å)/bond angle (°)
Ru(1)–O(1)	2.061(2)
Ru(1)–O(2)	2.060(2)
Ru(1)–N(1)	2.070(3)
Ru(1)–N(2)	2.079(3)
Ru(1)–N(3)	1.998(3)
Ru(1)–N(4)	2.001(3)
C(20)–N(3)	1.303(5)
C(21)–N(4)	1.318(5)
O(1)–Ru(1)–N(1)	80.31(9)
O(2)–Ru(1)–N(2)	80.33(9)
N(3)–Ru(1)–N(4)	78.8(1)
C(20)–N(3)–C(19)	119.8(3)
C(21)–N(4)–C(22)	119.1(4)
N(3)–C(20)–C(21)	115.5(4)
N(4)–C(21)–C(20)	115.4(3)

Table 5
Selected bond lengths (Å) and bond angles (°) of **6a** and **6b** (co-crystallized)

Isomer	Bond	Distance (Å)/angle (°)
cis,trans (**6a**)	Ru(1)–O(1)	2.082(2)
	Ru(1)–O(2)	2.0876(18)
	Ru(1)–N(1)	2.106(2)
	Ru(1)–N(2)	2.0825(19)
	Ru(1)–C(20)	2.190(3)
	Ru(1)–C(21)	2.189(2)
	Ru(1)–C(23)	2.170(3)
	Ru(1)–C(24)	2.169(3)
	C(20)–C(21)	1.378(4)
	C(23)–C(24)	1.381(4)
	O(3)–Ru(2)–O(4)	160.08(9)
	N(3)–Ru(2)–N(4)	91.68(8)
trans,cis (**6b**)	Ru(2)–O(3)	2.071(2)
	Ru(2)–O(4)	2.0760(17)
	Ru(2)–N(3)	2.112(2)
	Ru(2)–N(4)	2.121(2)
	Ru(2)–C(45)	2.192(3)
	Ru(2)–C(46)	2.190(2)
	Ru(2)–C(48)	2.160(2)
	Ru(2)–C(49)	2.172(2)
	C(45)–C(46)	1.380(4)
	C(48)–C(49)	1.374(4)
	O(3)–Ru(1)–O(4)	94.62(8)
	N(3)–Ru(1)–N(4)	152.75(8)

the interaction between the close-shelled [RuQ_2] core and the 2,5-norbornadiene ligand for both complexes.

3. Results and discussion

3.1. Synthesis and characterization of Ru^{III} Q_3

The synthesis of RuQ_3 (**1a**) and Ru(Me-Q)$_3$ (**1b**) from $RuCl_3 \cdot x$-H_2O have been reported [23a]. In this work we have reinvestigated the synthesis and have developed a general and high yield (>75%) method for the preparation a series of tris(8-quinolinolato)ruthenium(III) complexes, including **1a**, **1b**, and Ru(Cl-Q)$_3$ (**1c**). This method involves the reaction of Ru(acac)$_3$ with the neat ligand at 180 °C followed by chromatographic purification. The excess ligand can be readily recovered by sublimation.

The UV–Vis spectra of **1a** and **1b** are similar to those reported in the literature [23]. The X-ray crystal structure of RuQ_3 has been recently reported, which shows that the compound has a *meridonal* configuration [23b].

The cyclic voltammograms of **1a–c** exhibit two reversible couples which are assigned to $Ru^{IV/III}$ and $Ru^{III/II}$ couples. The redox potentials for **1a** and **1b** are similar to those reported in the literature [23]. As expected the redox potentials follow the order **1b** > **1a** > **1c**, i.e. the potentials increase with the electron-donating ability of the substituent.

3.2. Synthesis and characterization of bis(8-quinolinolato)ruthenium (II) complexes

Compound **1a** is a convenient starting material for the synthesis of a variety of bis(8-quinolinolato)ruthenium(II) complexes containing π-acceptor ligands, including dimethylsulfoxide (dmso), 4-picoline (pic), dienes and diazadiene, as outlined in Scheme 1. The general synthetic method involves reduction of **1a** with zinc amalgam in the presence of excess π-acceptor ligand in refluxing ethanol under argon. These compounds have been characterized by elemental analysis, IR and ^{1}H NMR, and the data are consistent with the proposed formulae. For an octahedral complex of the type Ru(Q)$_2$L$_2$ where the two L ligands are *cis*, there are three possible geometric isomers, as shown in Scheme 2:

3.2.1. $Ru^{II}Q_2(dmso)_2$

The ^{1}H NMR spectrum of $Ru^{II}Q_2$(dmso)$_2$ (**2**) shows that the methyl protons (2.974 and 2.660 ppm) of the two dmso ligands are chemically non-equivalent. The ratio between the integrals in the aromatic and the aliphatic regions is 1:1, consistent with the proposed formula. In the IR spectrum, a strong band occurs at 1078 cm^{-1}, which is in the region expected for S=O stretch of S-bonded ruthenium(II) dmso complexes (1020–1134 cm^{-1}) [42b,42c,42d,42e]. The S=O stretch for O-bonded ruthenium(II) dmso complexes occur at lower wavelengths (885–954 cm^{-1}) [42c,42d,42e].

The structure of **2** was established by X-ray crystallography. Fig. 1 shows a perspective view of the molecule. Selected bond lengths and bond angles are shown in Table 2. The two quinolinolato ligands adopt a *trans,cis* configuration, and the two *cis* dmso ligands are S-bonded to the ruthenium center. The two Ru–S(dmso) (2.224(5) and 2.233(5) Å) and S–O (1.457(13) and 1.481(12) Å) bond distances are comparable to those in other Ru(II) dmso complexes (2.241–2.364 Å and 1.459–1.50 Å, respectively) [42]. The Ru–N(Q) distances (2.07(1) Å and 2.08(2) Å) are similar to those in RuQ_3 (2.0527–2.0742 Å) [23b], but the Ru–O(Q) distances (2.077(12) and 2.094(11) Å) are slightly longer than those in RuQ_3 (1.9932–2.0392 Å) [23b] and is consistent with the lower atomic charge on the ruthenium (II) center.

This complex in 77K EtOH/MeOH glass is found to show a long lived ($\tau_0 = 439$ μs) emission at *ca.* 594 nm upon excitation with $\lambda = 300$ nm (Fig. 2). This emission are tentatively assigned as originated from the metal-perturbed intraligand (IL) π to π* phosphorescence derived from quinolate moieties mixed with the triplet metal-to-ligand charge transfer (MLCT) [dπ(Ru) to π*(Q)] character, similar to those reported in the related PtQ_2, IrQ3 and PbQ_2 systems [20]. The strong spin–orbit coupling introduced by the ruthenium metal center enhances the accessibility of the ^{3}IL excited states. The long-lived lifetime in the microsecond range is also indicative of its triplet parentage.

The cyclic voltammogram of **2** exhibits a quasi-reversible couple at 0.31 V (versus Fc$^{+/0}$).

3.2.2. $Ru^{II}Q_2(pic)_2$

Reduction of **1a** with zinc amalgam in the presence excess 4-picoline (pic) in refluxing ethanol produced a green crystalline solid. Elemental analysis and ^{1}H NMR spectroscopy are consistent with the formula $Ru^{II}Q_2$(pic)$_2$ (**3**).

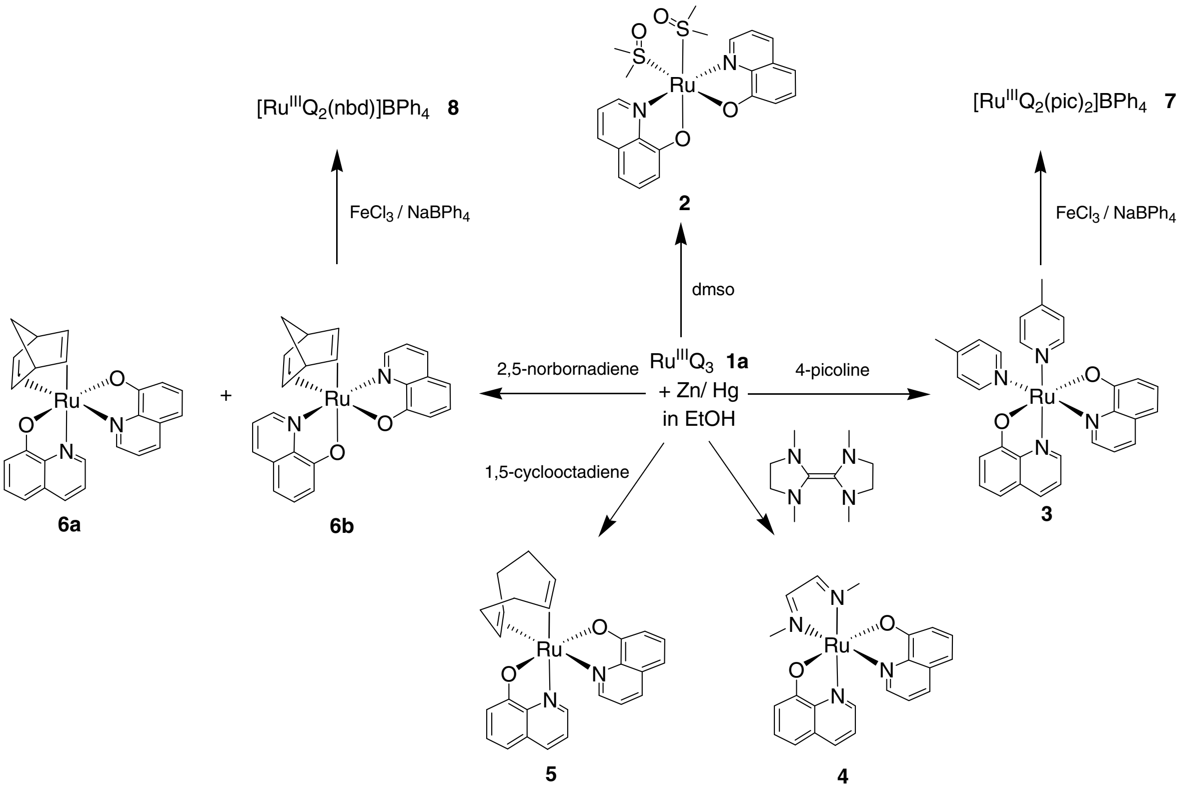

Scheme 1. Reactions of RuQ_3 (**1a**) with various π-acceptor ligands under reducing condition.

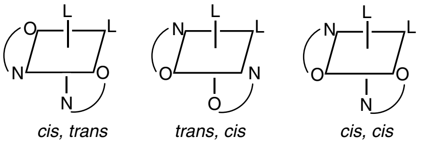

Scheme 2. Three possible geometric isomers of the complex RuQ_2L_2.

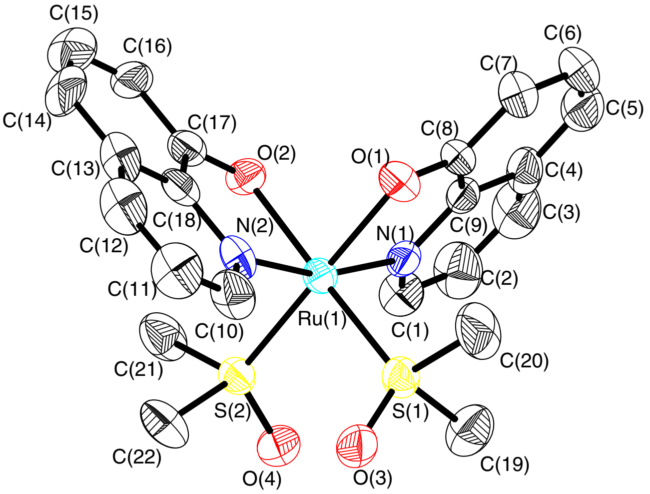

Fig. 1. ORTEP drawing of **2**, thermal ellipsoids are drawn at the 50% probability (hydrogen atoms are omitted for clarity).

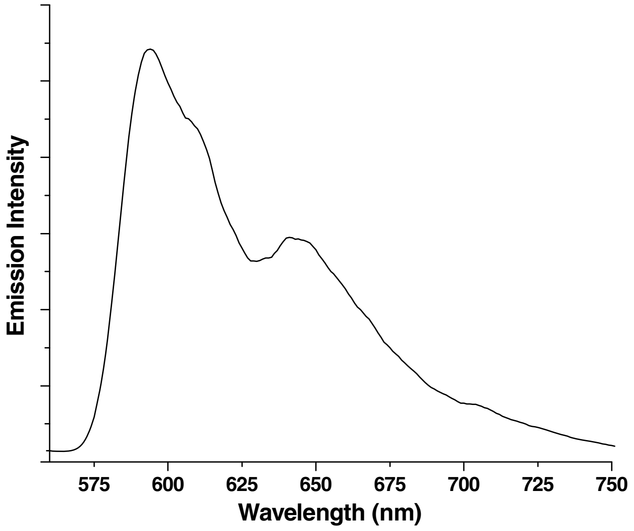

Fig. 2. Emission spectrum of **2** in ethanol/methanol (4:1) glass 77 K.

The X-ray crystal structure of **3** shows that the two quinolinolato ligands have a *cis,trans* configuration, in contrast to the *trans,cis* arrangement in **2**, and the two picoline ligands are *cis* (Fig. 3). The Ru–N(picoline) distances of 2.079(5) and 2.059(5) Å (Table 3) are similar to those in *trans*-$[Ru^{II}(phen)_2(py)_2][PF_6]_2$ (2.097(5) Å), and *trans*-$Ru^{II}(CN)_2(py)_4$ (2.090(4)–2.093(4) Å) [43]. The Ru–N(Q) and Ru–O(Q) distances (2.024(5), 2.040(5) and 2.080(4), 2.095(4) Å, respectively) are similar to those in **2.**

The cyclic voltammogram of **3** (Fig. 4) exhibits a reversible couple at −0.56 V and a quasi-reversible couple at 0.56 V (versus $Fc^{+/0}$), which are assigned to $Ru^{III/II}$ and $Ru^{IV/III}$ couples, respectively.

3.2.3. $Ru^{II}Q_2(dab)$

Bis(1,3-dialkylimidazolidin-2-ylidene) has been used as a carbene precursor for the preparation of various transition metal carbene complexes [44]. Attempts were made to prepare a carbene

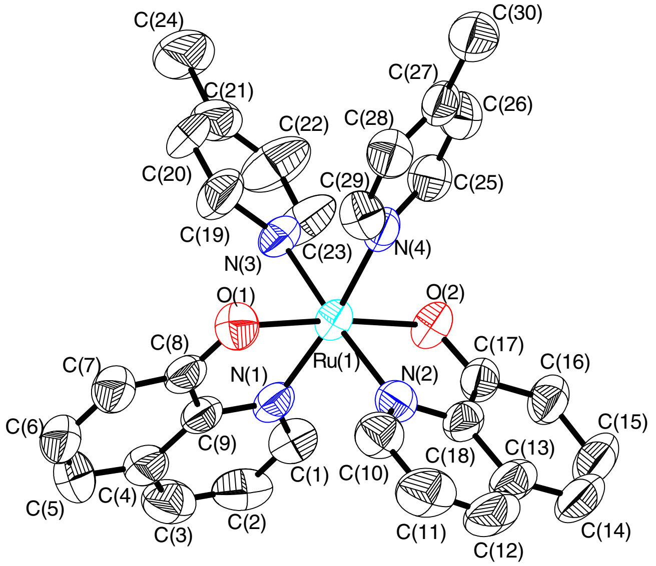

Fig. 3. ORTEP drawing of **3**, thermal ellipsoids are drawn at the 50% probability (hydrogen atoms are omitted for clarity).

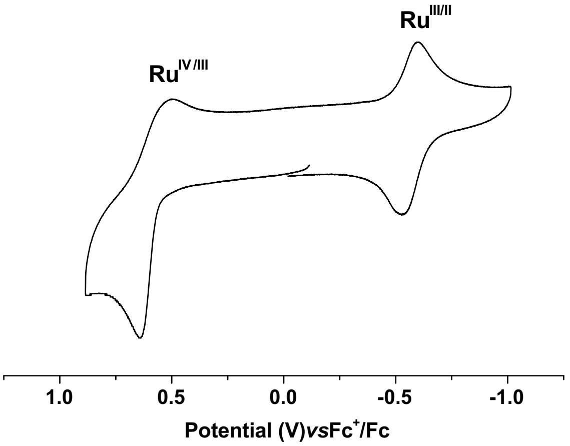

Fig. 4. Cyclic voltammogram of **3** (0.1 M [NBu$^n_4$]PF$_6$ in CH$_3$CN).

complex of Ru^{II}Q$_2$ by treatment of **1a** with bis(1,3-dimethylimidazolidin-2-ylidene) (L′) in the presence of Zn/Hg under argon. A purple solution was produced, but attempts to isolate pure products from this solution were unsuccessful. However, the purple solution readily turned red upon exposure to air, and the red complex RuQ$_2$(dab) (**4**) (dab = *N*,*N*′-dimethyl-1,4-diazabuta-1,3-diene) could be isolated. The reaction presumably occurs by initial formation of RuQ$_2$L′, followed by cleavage and oxidation of L′. Attempts to prepare **4** by using *N*,*N*′-dimethylethylenediamine (Me$_2$en) instead of L′ were unsuccessful, neither RuQ$_2$(Me$_2$en) nor **4** could be isolated. Although there are numerous examples of ruthenium 1,4-diaza-1,3-butadiene complexes containing bulky substituents such as isopropyl, *tert*-butyl and cyclohexyl on the imine nitrogen [45], this is the first example of a ruthenium complex containing the methyl-substituted diazabutadiene ligand.

The X-ray structure shows that the two quinolinolato ligands are coordinated to the ruthenium center in a *cis*,*trans* fashion, similar to **3**; and the dab ligand functions as a bidentate ligand (Fig. 5). Selected bond distances and bond angles are shown in Table 4. The Ru–N(Q) (2.070(3) and 2.079(3) Å) and Ru–O(Q) (2.061(2) and 2.060(2) Å) distances are similar to those in **2** and **3**. The Ru(1)–N(dab) distances (1.998(3) and 2.001(3) Å) are among the shortest in ruthenium(II) diazabutadiene complexes (2.01–2.15 Å) [45]. The imine bond distances (N(4)–C(21) and N(3)–C(20)) (1.303(5) and 1.318(5) Å) are within the reported range for other ruthenium(II) diazabutadiene complexes (1.25(1)–1.34(2) Å) [45]. The C(21)–N(4)–C(22) and C(20)–N(3)–C(19) bond angles (119.1(4) and 119.8(3)) are consistent an sp^2 imine nitrogen.

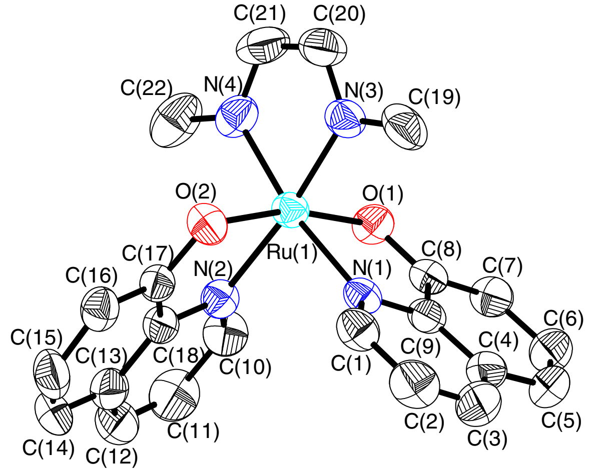

Fig. 5. ORTEP drawing of **4**, thermal ellipsoids are drawn at the 50% probability (hydrogen atoms are omitted for clarity).

The cyclic voltammogram of **4** shows a reversible Ru$^{III/II}$ couple at 0.77 V (versus Fc$^{+/0}$) (Fig. 6). Two reversible couples also appear at $E = -1.64$ and -1.80 V, these are assigned as the dab$^{0/-}$ and dab$^{-/2-}$ couples [46].

3.2.4. *Ru^{II}Q$_2$(COD)*

The synthesis and X-ray crystal structure of this compound have been reported recently [24]. The two quinolinolato ligands adopt a *cis*,*trans* configuration. The reported synthesis uses [Ru(COD)Cl$_2$]$_2$ as the starting material. In this work the same compound has been prepared from RuQ$_3$, the spectroscopic properties agree with that prepared from [Ru(COD)Cl$_2$]$_2$.

3.2.5. *Ru^{II}Q$_2$(nbd)*

The reaction of RuQ$_3$ with 2,5-norbornadiene (nbd) in ethanol in the presence of zinc amalgam produces a mixture of red and yellow crystalline solids. Elemental analysis of both solids are

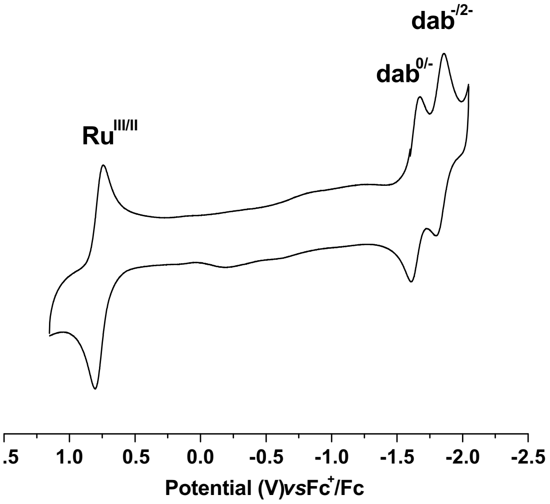

Fig. 6. Cyclic voltammogram of **4** (0.1 M [NBu$^n_4$]PF$_6$ in CH$_3$CN).

consistent with the formula $RuQ_2(nbd)$. X-ray crystallography showed that the yellow compound is the *cis,trans* isomer (**6a**), whereas as the red crystals consist of co-crystallized *cis,trans* (**6a**) and *trans,cis* (**6b**) isomers (Fig. 7). The bond distances and angles for **6a** in the red and yellow crystals are the same (Table 5). The bond distances for **6a** are also very similar to those for **6b**. The Ru–C(nbd) distances for **6a** and **6b** (2.160(2)–2.192(3) Å) are within the range for other ruthenium 2,5-norbornadiene complexes (2.150–2.220 Å) [47]. The olefinic C═C distances in **6a** and **6b** (1.374(4)–1.381(4) Å) are also comparable to those in other ruthenium 2,5-norbornadiene complexes (1.383–1.401 Å) [47], and are longer than the length of 1.35 Å in the free olefin [47d], reflecting the existence of ruthenium–olefin π-back bonding.

The mixture of **6a** and **6b** in the red crystals can be readily separated by column chromatography (neutral alumina) as yellow and red solids. The ^1H NMR spectra of both compounds have a ratio of 3:2 for the integrals in the aromatic and the aliphatic regions, consistent with the presence of two 8-quinolinolato ligands and a 2,5-norbornadiene ligand. In the UV–Vis spectrum the lowest energy absorption band for **6a** occurs at 427 nm, while that of **6b** occurs at a lower wavelength of 500 nm (Fig. 8).

The cyclic voltammogram of **6b** in CH_3CN shows a reversible couple at −0.03 V and a quasi-reversible couple at 0.83 V versus $Fc^{+/0}$ which are assigned to the $Ru^{III/II}$ and the $Ru^{IV/III}$ couples, respectively (Fig. 9). In contrast, **6a** shows only a quasi-reversible $Ru^{III/II}$ couple at $E_{pa} = 0.41$ V and no $Ru^{IV/III}$ couple in the same potential range (−1.0–1.0 V). However, there is a relatively small couple at 0.64 V, which presumably is due to $[RuQ_2(CH_3CN)_2]^{2+/+}$ generated from loss of the alkene ligand from **6a** upon oxidation to Ru^{III}.

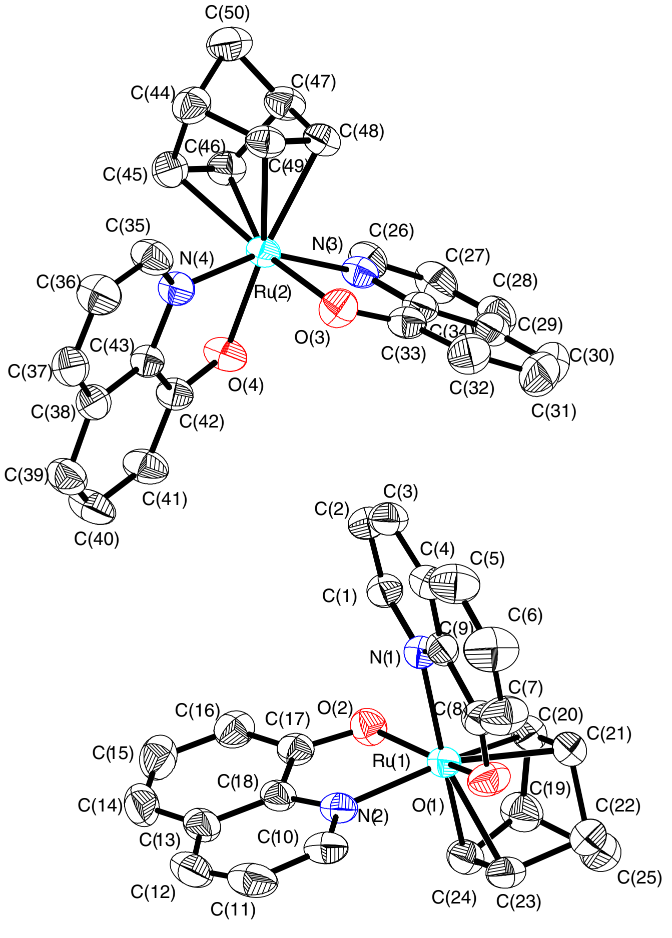

Fig. 7. ORTEP drawing of co-crystallized **6a** (bottom) and **6b** (top) in the red crystals, thermal ellipsoids are drawn at the 50% probability (hydrogen atoms are omitted for clarity).

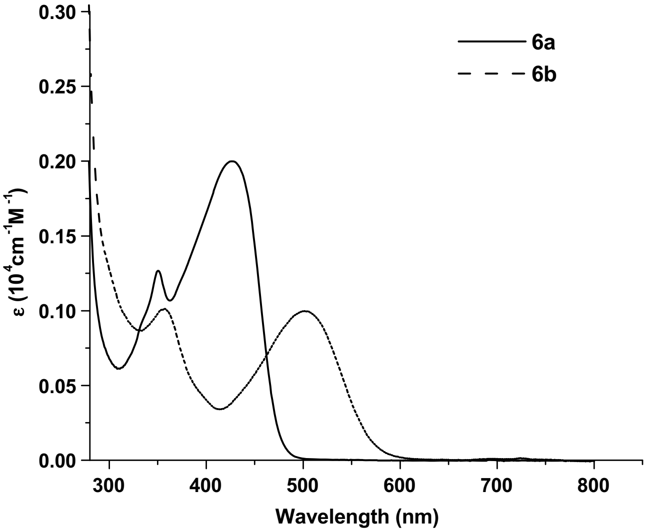

Fig. 8. UV–Vis spectra of **6a** and **6b**.

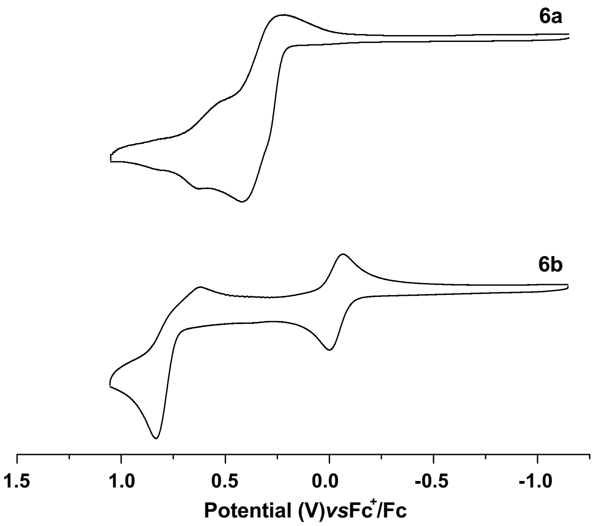

Fig. 9. Cyclic voltammogram of **6a** and **6b**.

Since **6a** and **6b** have similar bond lengths and angles but differ significantly in redox potentials and energies of electronic transitions, theoretical calculations have been performed on these two compounds in order to gain an insight into the nature of these differences. The ground-state structures of complexes **6a** and **6b** were optimized at the DFT level (B3LYP). Their optimized structural data are in satisfactory agreement with their X-ray crystal structure data. The highest-occupied molecular orbitals (HOMOs) for both complexes are mainly contributed from the d orbitals of Ru(II) and the orbitals of Q (**6a**, 19.8% d(Ru), 71.3% Q; **6b**, 30.1% d(Ru), 59.7% Q). It is noted that the energy of the HOMO of **6a** (−4.82 eV) is lower than that of **6b** (−4.41 eV) by 0.41 eV. This is consistent with the experimental findings that (i) the first oxidation wave for **6a** ($E_{pa} = 0.41$ V versus $Fc^{+/0}$) is more anodic than that of **6b** ($E_{1/2} = -0.03$ V versus $Fc^{+/0}$); (ii) the lowest energy transition (presumably due to dπ[Ru(II)] to π^* (Q) MLCT transition) of **6a**

(λ_{max} = 427 nm) is blue-shifted compared to **6b** (λ_{max} = 500 nm) by 0.42 eV. Charge decomposition analysis (CDA) calculations suggest that the bonding interaction of the close-shelled [RuQ_2] moiety and the nbd ligand for both complexes can be described by the Dewar–Chatt–Duncanson donor–acceptor model as the residual terms (Δ) are essentially zero (**6a**, −0.027; **6b**, −0.022). The ratio of the values for [nbd → Ru^{2+}] donation (d) and [Ru^{2+} → nbd] back-donation (b), d/b, are 2.00 and 1.72 for **6a** and **6b**, respectively, suggesting an overall charge donation from nbd to the Ru^{2+} centers, although the Ru^{2+} centers are supported by the electron-donating ligands Q.

3.3. Synthesis and characterization of bis(8-quinolinolato)ruthenium (III) complexes

3.3.1. [$Ru^{III}Q_2(pic)_2$]BPh_4

In accordance with its relatively low $Ru^{III/II}$ redox potential ($E_{1/2}$ = 0.56 V versus $Fc^{+/0}$), a solution of **3** in chloroform was oxidized within minutes by air at room temperature. Oxidation of **3** can be efficiently carried out by $FeCl_3$ in methanol in the presence of excess $NaBPh_4$ to give a dark green crystalline solid, formulated as [$Ru^{III}Q_2(pic)_2$]BPh_4 (**7**). Compound **7** has a room temperature magnetic moment of μ_{eff} = 2.04 μ_B (Gouy method), consistent with a low-spin d^5 Ru^{III} complex. The ESI/MS in dichloromethane shows peaks at m/z = 576, 483 and 390 which is due to $[M]^+$, $[M\text{-pic}]^+$ and $[M\text{-2pic}]^+$, respectively. The cyclic voltammogram of **7** is the same as that of **3**, suggesting that no isomerization has occurred during the oxidation.

3.3.2. [$Ru^{III}Q_2(nbd)$]BPh_4

In accordance with its redox potential ($E_{1/2}$ = 0.03 V versus $Fc^{+/0}$), **6b** can be readily oxidized by $FeCl_3$ in methanol in the presence of excess $NaBPh_4$ to give a dark brown crystalline solid formulated as [$Ru^{III}Q_2(nbd)$]BPh_4 (**8**). As expected, no reaction occurred when **6a** (E_{pa} = 0.41 V versus $Fc^{+/0}$) was treated with $FeCl_3$. Compound **8** has a room temperature magnetic moment of μ_{eff} = 2.2 μ_B (Gouy method), consistent with a low-spin d^5 Ru^{III} complex. The ESI/MS of **8** shows $[M]^+$ at m/z = 482, there is also a minor peak at 390 which is due to $[M\text{-nbd}]^+$.

This is a rare example of a stable ruthenium(III) alkene complex. Ruthenium (III) alkene complexes are usually unstable with respect to loss of alkene, unless another donor atom is also present to form a stable chelate [48]. Presumably Q^- is sufficiently electron-donating so that there is some π-back bonding between Ru^{III} and the alkene. Another example of ruthenium(III) norbornadiene complex, [$Ru(Et_2dtc)_2(nbd)$](I_3), has been reported recently; where Et_2dtc is *N*,*N*-diethyldithiocarbamate [47d].

Since the 2,5-norbornadiene is coordinated to a ruthenium(III) center, it is expected to be electrophilic. However, reaction of **8** with various nucleophiles (R_2NH, CN^-) invariably resulted in the reduction of **8** back to **6b**, as monitored by UV–Vis spectroscopy. When reactions were carried out on a preparatory scale, **6b** could be isolated in >90% yields. Even on standing, a dark purple solution of **8** in CH_2Cl_2 gradually turned to orange **6b** with a rate constant of 0.013 s^{-1} at 25.0 °C.

4. Conclusion

A general, high-yield synthetic method for RuQ_3 and its derivatives has been developed. RuQ_3 is a versatile starting material for the preparation of a variety of bis(8-quinolinolato)ruthenium(II) complexes containing π-acceptor ligands. The quinolinolato complexes adopt either *cis*, *trans* or *trans,cis* configurations. In the case of $RuQ_2(nbd)$ (**6**) both isomers have been isolated and structurally characterized. These two isomers have significantly different properties including redox potentials and energies of electronic transitions, despite their very similar bond distances. A novel ruthenium(III) norbornadiene complexes [$RuQ_2(nbd)$]BPh_4 has also been isolated, indicating that there is a rich coordination chemistry of ruthenium with 8-hydroxyquinoline.

Acknowledgements

The work described in this paper was supported by the Research Grants Council of Hong Kong (CityU 101403) and the City University of Hong Kong (7001925).

Appendix A. Supplementary material

CCDC 670792, 670793, 670794, 670795 and 670796 contain the supplementary crystallographic data for **2**, **3**, **4**, **6** and **6a**. These data can be obtained free of charge from The Cambridge Crystallographic Data Centre via www.ccdc.cam.ac.uk/data_request/cif. Supplementary material such as spectral data for **7** and **8**; electrochemical data for **1–6**; crystal data and selected bond lengths and bond angles of **6a** are also available. Supplementary data associated with this article can be found, in the online version, at doi:10.1016/j.ica.2008.05.036.

References

[1] R.G.W. Hollingshead, Oxine and its Derivatives, vols. I–IV, Butterworths, London, 1954–1956.
[2] E.B. Sandell, H. Onishi, Photometric Determination of Traces of Metals, General Aspects; Fourth Edition of Part I of Colorimetric Determination of Traces of Metals, Wiley, New York, 1978, p. 415.
[3] R. Ballardini, G. Varani, M.T. Indelli, F. Scandola, Inorg. Chem. 25 (1986) 3858.
[4] C. Bartocci, S. Sostero, O. Traverso, A. Cox, T.J. Kemp, W.J. Reed, J. Chem. Soc., Faraday Trans. 76 (1980) 797.
[5] K. Soroka, R.S. Vithanage, D.A. Phillips, B. Walker, P.K. Dasgupta, Anal. Chem. 59 (1987) 629.
[6] M.A. Palacios, Z. Wang, V.A. Montes, G.V. Zyryanov, B.J. Hausch, K. Jursíková, P. Anzenbacher Jr., Chem. Commun. (2007) 3708.
[7] T. Moeller, A.J. Cohen, J. Am. Chem. Soc. 72 (1950) 3546.
[8] W.E.J. Ohnesorge, Inorg. Nucl. Chem. 29 (1967) 485.
[9] C.H. Chen, J. Shi, Coord. Chem. Rev. 171 (1998) 161.
[10] P.E. Burrows, L.S. Sapochak, S.R. Forrest, Appl. Phys. Lett. 64 (1994) 2718.
[11] Y. Wang, W. Zhang, Y. Li, L. Ye, G. Yang, Chem. Mater. 11 (1999) 530.
[12] W. Humbs, E. Veldhoven, H. Zhang, M. Glasbeek, Chem. Phys. Lett. 304 (1999) 10.
[13] Z. Chen, J. Yu, M. Sone, S. Miyata, Y. Lu, T. Watanabe, J. Phys. D: Appl. Phys. 34 (2001) 2679.
[14] W. Stampor, J. Kalinowski, G. Marconi, P. Di Marco, V. Fattori, G. Giro, Chem. Phys. Lett. 283 (1998) 373.
[15] L. Wang, X. Jiang, Z. Zhang, S. Xu, Displays (2000) 47.
[16] O.M. Khreis, R.J. Curry, M. Somerton, W.P.J. Gillin, Appl. Phys. 88 (2000) 777.
[17] R.J. Curry, W.P. Gillin, Synth. Met. (2000) 35.
[18] O.M. Khreis, W.P. Gillin, M.P.M. Somerton, R.J. Curry, Org. Electron. 2 (2001) 45.
[19] R.J. Curry, W.P. Gillin, Appl. Phys. Lett. 75 (1999) 1380.
[20] R. Ballardini, G. Varani, M.T. Indelli, F. Scandola, Inorg. Chem. 25 (1986) 3858.
[21] D. Donges, J.K. Nagle, H. Yersin, Inorg. Chem. 36 (1997) 3040.
[22] C. Bartocci, S. Sostero, O. Traverso, J.C.S. Faraday I 76 (1980) 797.
[23] (a) G.K. Lahiri, S. Bhattacharya, B.K. Ghosh, A. Charkravorty, Inorg. Chem. 26 (1987) 4324;
(b) J.G. Małecki, M. Jaworska, R. Kruszynski, J. Kłak, Polyhedron 24 (2005) 3012;
(c) S.G. Rodman, J.K. Nagle, Inorg. Chim. Acta 105 (1985) 205.
[24] (a) P.J. Powell, Organomet. Chem. 65 (1974) 89;
(b) C. Slugovc, A. Koppitz, A. Pogantsch, F. Stelzer, Inorg. Chim. Acta 358 (2005) 2718.
[25] M. Menon, A. Pramanik, N. Bag, A. Charkravorty, J. Chem. Soc., Dalton Trans. (1995) 1417.
[26] J.T. Warren, W. Chen, D.H. Johnston, C. Turro, Inorg. Chem. 38 (1999) 6187.
[27] W.P. Griffith, D. Pawson, J. Chem. Soc., Dalton. Trans. (1973) 1315.
[28] H.E. Winberg, Chem. Abstr. 64 (1966) 15854h.
[29] DIRDIF 92: P.T. Beurskens, G. Admiraal, W.P. Bosman, S. Garcis-Granda, R.O. Gould, J.M.M. Smits, C. Smykalla, PATTY: The DIRDIF Program System, Technical Report of the Crystallography Laboratory, University of Nijmegen, The Netherlands, 1992.
[30] A. Altomare, G. Cascarano, C. Giacovazzo, A. Guagliardi, J. Appl. Crystallogr. 26 (1993) 343.
[31] G.M. Sheldrick, Acta Crystallogr., Sect. A 46 (1990) 467.

[32] DIRDIF 94: P.T. Beurskens, G. Admiraal, G. Beurskens, W.P. Bosman, R. de Gelder, R. Israel, J.M.M. Smits, The DIRDIF 94 Program System, Technical Report of the Crystallography Laboratory, University of Nijmegen, The Netherlands, 1994.

[33] DIRDIF 99: P.T. Beurskens, G. Admiraal, G. Beurskens, W.P. Bosman, R. de Gelder, R. Israel, J.M.M. Smits, The DIRDIF 99 Program System, Technical Report of the Crystallography Laboratory, University of Nijmegen, The Netherlands, 1999.

[34] CRYSTALSTRUCTURE 3.00: Crystal Structure Analysis Package, Rigaku and Rigaku/MSC, 2000–2002.

[35] TEXSAN: Crystal Structure Analysis Package, Molecular Structure Corporation, The Woodlands, TX, USA, 1985 and 1992.

[36] A.D. Becke, J. Chem. Phys. 98 (1993) 5648.

[37] C. Lee, W. Yang, R.G. Parr, Phys. Rev. B 37 (1988) 785.

[38] M. Dolg, H. Stoll, H. Preuss, R.M. Pitzer, J. Phys. Chem. 97 (1993) 5852.

[39] M.M. Francl, W.J. Pietro, W.J. Hehre, J.S. Binkley, M.S. Gordon, D.J. DeFrees, J.A. Pople, J. Chem. Phys. 77 (1982) 3654.

[40] M.J. Frisch, G.W. Trucks, H.B. Schlegel, G.E. Scuseria, M.A. Robb, J.R. Cheeseman, J.A. Montgomery Jr., T. Vreven, K.N. Kudin, J.C. Burant, J. Millam, S.S. Iyengar, J. Tomasi, V. Barone, B. Mennucci, M. Cossi, G. Scalmani, N. Rega, G.A. Petersson, H. Nakatsuji, M. Hada, M. Ehara, K. Toyota, R. Fukuda, J. Hasegawa, M. Ishida, T. Nakajima, Y. Honda, O. Kitao, H. Nakai, M. Klene, X. Li, J.E. Knox, H.P. Hratchian, J.B. Cross, V. Bakken, C. Adamo, J. Jaramillo, R. Gomperts, R.E. Stratmann, O. Yazyev, A.J. Austin, R. Cammi, C. Pomelli, J.W. Ochterski, P.Y. Ayala, K. Morokuma, G.A. Voth, P. Salvador, J.J. Dannenberg, V.G. Zakrzewski, S. Dapprich, A.D. Daniels, M.C. Strain, O. Farkas, D.K. Malick, A.D. Rabuck, K. Raghavachari, J.B. Foresman, J.W. Ortiz, Q. Cui, A.G. Baboul, S. Clifford, J. Cioslowski, B.B. Stefanov, G. Liu, A. Liashenko, P. Piskorz, I. Komaromi, R.L. Martin, D.J. Fox, T. Keith, M.A. Al-Laham, C.Y. Peng, A. Nanayakkara, M. Challacombe, P.M.W. Gill, B. Johnson, W. Chen, M.W. Wong, C. Gonzalez, J.A. Pople, GAUSSIAN 03, Revision D.01, Gaussian, Inc., Wallingford CT, 2004.

[41] (a) G. Frenking, N. Fröhlich, Chem. Rev. 100 (2000) 717;
(b) S. Dapprich, G. Frenking, J. Phys. Chem. 99 (1995) 9352.

[42] (a) A.A. Rachford, J.L. Petersen, J.J. Rack, Inorg. Chem. 45 (2006) 5953;
(b) E. Reisner, V.B. Arion, M.F.C. Guedes da Silva, R. Lichtenecker, A. Eichinger, B.K. Keppler, V.Y. Kukushkin, A.J.L. Pombeiro, Inorg. Chem. 43 (2004) 7083;
(c) E. Alessio, G. Mestroni, G. Nardin, W.M. Attia, M. Calligaris, G. Sava, S. Zorzet, Inorg. Chem. 27 (1988) 4099;
(d) E. Alessio, B. Milani, M. Bolle, G. Mestroni, P. Faleschini, S. Geremia, M. Calligaris, Inorg. Chem. 34 (1995) 4712;
(e) E. Alessio, B. Milani, M. Bolle, G. Mestroni, P. Faleschini, F. Todone S. Geremia, M. Calligaris, Inorg. Chem. 34 (1995) 4722;
(f) T.J. Beasley, R.D. Brost, C.K. Chu, S.L. Grundy, S.R. Stobart, Organometallics 12 (1993) 4599;
(g) B.J. Coe, T.J. Meyer, P.S. White, Inorg. Chem. 32 (1993) 4012;
(h) D. Sellmann, J. Utz, F.R. Heinemann, Inorg. Chem. 38 (1999) 5314.

[43] (a) P. Bonneson, J.L. Walsh, W.T. Pennington, A.W. Cordes, B. Durham, Inorg. Chem. 22 (1983) 1761;
(b) P. Desjardins, G.P.A. Yap, R.J. Crutchley, Inorg. Chem. 38 (1999) 5901;
(c) B.J. Coe, T.J. Meyer, P.S. White, Inorg. Chem. 34 (1995) 3600.

[44] (a) P.B. Hitchcock, M.F. Lappert, P.L. Pye, J. Chem. Soc., Chem. Commun. (1976) 644;
(b) P.B. Hitchcock, M.F. Lappert, P.L. Pye, J. Chem. Soc., Chem. Commun. (1974) 679;
(c) P.B. Hitchcock, M.F. Lappert, P.L. Pye, J. Chem. Soc., Chem. Commun. (1977) 196.

[45] (a) L.H. Staal, L.H. Polm, K. Vrieze, F. Ploeger, C.H. Stam, Inorg. Chem. 20 (1981) 3590;
(b) C.J. Kleverlaan, D.J. Stufkens, J. Fraanje, K. Goubitz, Eur. J. Inorg. Chem. (1998) 1243;
(c) M.P. Aarnts, M.P. Wilms, K. Peelen, J. Fraanje, K. Goubitz, F. Hartl, D.J. Stufkens, J.B. Baerends, A. Vlcek, Inorg. Chem. 35 (1996) 5468;
(d) B. de Klerk-Engel, J.G.P. Delis, K. Vrieze, Organometallics 13 (1994) 3269;
(e) M.P. Aarnts, D.J. Stufkens, A. Oskam, J. Fraanje, K. Goubitz, Inorg. Chim. Acta 256 (1997) 93;
(f) B. de Klerk-Engel, J.G.P. Delis, J. Ernsting, C.J. Elsevier, Frühauf, D.J. Stufkens, K. Vrieze, K. Goubitz, J. Fraanje, Inorg. Chim. Acta 250 (1995) 273.

[46] (a) H.M. Tuononen, A.F. Armstrong, Dalton Trans. (2006) 1885;
(b) H.M. Tuononen, A.F. Armstrong, Inorg. Chem. 44 (2005) 8277.

[47] (a) D.C. Wilson, J.H. Nelson, J. Organomet. Chem. 682 (2003) 272;
(b) T. Hayashida, K. Miyazaki, Y. Yamaguchi, H. Nagashima, J. Organomet. Chem. 634 (2001) 167;
(c) J. Sutter, S.L. James, P. Steenwinkel, T. Karlen, D.M. Grove, N. Veldman, W.J.J. Smeets, A.L. Spek, G. van Koten, Organometallics 15 (1996) 941;
(d) W.H. Leung, J.L.C. Chim, H. Hou, T.S.M. Hun, I.D. Williams, W.T. Wong, Inorg. Chem. 36 (1997) 4432;
(e) K. Itoh, N. Oshima, G.B. Jameson, H.C. Lewis, J. Ibers, J. Am. Chem. Soc. 103 (1981) 3014.

[48] M.A. Bennett, G.A. Heath, D.C.R. Hockless, I. Kovacik, A.C. Willis, J. Am. Chem. Soc. 120 (1998) 932.